

# Direct visualization of walking motions of photocontrolled nanomachine on the DNA nanostructure

*Yangyang Yang,<sup>†‡</sup> Marisa Goetzfried,<sup>‡¶</sup> Kumi Hidaka,<sup>‡</sup> Mingxu You,<sup>§¶</sup> Weihong Tan,<sup>\* §¶</sup>*

*Hiroshi Sugiyama<sup>\*†‡</sup> and Masayuki Endo<sup>\*†</sup>*

<sup>†</sup>Institute for Integrated Cell-Material Sciences (WPI-iCeMS), Kyoto University, Yoshida-  
ushinomiya-cho, Sakyo-ku, Kyoto 606-8501, Japan

<sup>‡</sup>Department of Chemistry, Graduate School of Science, Kyoto University, Kitashirakawa-  
oiwakecho, Sakyo-ku, Kyoto 606-8502, Japan

<sup>§</sup>Molecular Science and Biomedicine Laboratory, State Key Laboratory of Chemo/Bio-Sensing  
and Chemometrics, College of Chemistry and Chemical Engineering, College of Biology,  
Collaborative Innovation Center for Molecular Engineering and Theranostics, Hunan University,  
Changsha, Hunan 410082, China

<sup>¶</sup>Department of Chemistry and Physiology and Functional Genomics, Center for Research at the  
Bio/Nano Interface, Shands Cancer Center, UF Genetics Institute, University of Florida,  
Gainesville, Florida 32611-7200

## ABSTRACT

A light-driven artificial molecular nanomachine was constructed based on DNA scaffolding. Pyrene-modified walking strands and disulfide bond-connected stator strands, employed as anchorage sites to support walker movement, were assembled into a 2D DNA tile. Pyrene molecules excited by photoirradiation at 350 nm induced cleavage of disulfide bond-connected stator strands, enabling the DNA walker to migrate from one cleaved stator to the next on the DNA tile. Importantly, the light-fuelled mechanical movements on DNA tile were firstly visualized in real time during UV irradiation using high-speed atomic force microscopy (HS-AFM).

Keywords DNA origami, light-driven, DNA motor, high-speed AFM, single molecule analysis

Remarkable strides have been made in single-molecule analysis of biomolecules, largely benefited by the development of various single-molecule techniques, such as atomic force microscopy (AFM) and super-resolution fluorescence microscopy.<sup>1-3</sup> AFM is able to examine single molecules at nanometer resolution, and the scanning can be easily carried out under physiological conditions.<sup>4</sup> It has already been applied to single-molecule imaging and to investigate interactions of molecules of interest.<sup>3</sup> Moreover, high-speed AFM allows for real-time observation of the dynamic behaviors of biological samples in a subsecond time scale, taking advantage of its fast scanning rate.<sup>5-7</sup> For observation at the nanoscale, precise locating and positioning of biomolecules and nanoparticles are required. The recent advent DNA origami<sup>8</sup> based on well-established DNA nanotechnology can serve as excellent scaffold for the functionalization with different kinds of molecules at predesigned positions and limited nanospace.

The direct visualization of dynamic interactions between multiple molecules has already been reported by combining DNA origami methods with high-speed AFM.<sup>4,9</sup> Most dynamic activities of biomolecules, such as chemical reactions,<sup>10</sup> structural changes of DNA strands,<sup>11-15</sup> mechanical movements,<sup>16,17</sup> can be characterized directly on nanometer-sized DNA structures under fast scanning rate of high-speed AFM. The continuous real-time behaviors of target molecules can be noted and captured in relatively high resolution. Our group have developed a series of DNA nanodevices for direct observation of photo-induced movements of single molecules in various DNA origamis<sup>11,18,19</sup> as well as the regulation of the assemble/disassemble of photo-controllable nanostructures<sup>19,20</sup>. Results indicate that light energy is easily implemented with nanometer-sized DNA nanostructures, especially on the surface of mica, which, with its ultra-flattened surface, affords equal photon distribution during observation and imaging.

Artificial DNA motors based on pre-constructed DNA scaffolds have already been developed, and the stepwise walking has also been captured in time-lapse images.<sup>16, 17, 21-23</sup> In general, these walking nanodevices were mostly fueled by enzymatic reaction or by external addition of counterpart strands, in which the programmed controllability is, for the most part, difficult to achieve and efficiency is also related to a limited energy supply. As a sustainable option, light source was anticipated to serve for DNA based nanomachines. A series of photosensitive molecules, such as the azobenzene- and pyrene-modified DNA motors were developed, allowing for DNA nanodevices under manual as well as remote control.<sup>24, 25</sup> Powered by light, the walker's movements were confirmed indirectly by gel electrophoresis and by fluorescence spectroscopy. However, the real-time mechanical movements of walking process driven by external photoirradiation have not been directly characterized yet. The stepwise mechanical motions of DNA walker on DNA tile have already been observed, which was initiated by the addition of nicking restriction enzyme.<sup>17</sup> The walking system has to be incubated with nicking restriction enzyme before the AFM scanning. Here we describe a light-driven DNA nanomachine able to walk along a linear track on a single 2D DNA tile. The dynamic movements during photoirradiation are directly visualized by high-speed AFM in real-time, for which the light-energy input can be introduced during the AFM scanning at any time.

As shown in Figure 1a (detailed design can be seen in Figure S1), the walking nanomachine contains two components: 1) a rectangular DNA tile as supporting scaffold where four anchorage sites are chosen for the elongation with stator strands (S1 to S4) and 2) a walking strand which can form the duplex with stator strands on the surface of the DNA tile. The walking strand consists of a shorter strand and a longer strand connected by an oligonucleotide modified with two pyrene molecules (All sequences can be seen in Table S1). And stator strand (S1, S2 and S3)

is composed of two strands connected by disulfide bond, in which S1 containing two extra bases to hybridize with the walker helps to bias the initial walker position.<sup>17</sup> S4 is designed as the walker's terminus, thus carrying three extra thymine bases, instead of the disulfide bond, to prevent the dissociation of the walker from the stator and to terminate its movement. All four stators (S1 to S4) with same facing orientation are arranged as a linear track and separated by a distance of ~ 6 nm on the DNA tile. Here the relatively short track (four stators) would help us to identify the location of walker promptly on the tile. Also long track is not utilized since it requires much longer time of irradiation, which might induce the photo damage.

It has been reported that excited pyrene molecules, as, for example, by photoirradiation, can efficiently facilitate cleavage of disulfide bond (dashed area of Figure. 1a) when pyrene and disulfide bond are in close proximity, e.g., the neighboring position in DNA duplex.<sup>26</sup> To distinguish the location of the walker-stator duplex, hairpin structures in a parallel arrangement along the both sides of the walking track were introduced separately as referencing position markers (Figures 1a and 2). One forward-step of the walker strand driven by photoirradiation is illustrated in Figure 1b. The disulfide bond is reduced by the electron transfer after the photoirradiation at 350 nm. The partially dissociated walker started to search for another accessible anchorage by the release of the cleaved stator strands. One-step forward motion is finally accomplished because of strand displacement reaction. The unidirectional stepping of the walker will keep on until the final step is completed under continuous photoirradiation. Here a "burnt bridge" mechanism<sup>27, 28</sup> is employed to control the unidirectional movement of the walker.

The preparation of the DNA walking system was followed two steps, including 1) assembly (annealing the solution from 85 °C to 15 °C at a rate of -1 °C/min) of the DNA tile by mixing single-stranded M13mp18 with staple strands containing stators of S2-S4 and 2) addition of

walker-S1 duplex into the purified DNA tile solution containing 20 mM Tris buffer (pH 7.6), 10 mM MgCl<sub>2</sub>, and 1 mM EDTA, followed by annealing from 35 °C to 15 °C at a rate of -0.05 °C/min. The assembled tile with the walker was then confirmed by AFM. AFM images in Figure 2a (also see Figure S1) show the walker-stator duplex at four anchorage sites on DNA tile separately, which are all clearly identified by using parallel hairpin DNAs as referencing markers.

Before introducing the photoirradiation, the distribution of the walker at four anchorage sites in the formation of walker-stator duplex on tile was examined by AFM imaging and further manual counting. The result is shown in Figure 2b (UV, 0 h, Table S2, Figure S2). It was initially found that ~ 65% of walker was successfully located at the starting position S1. From the AFM images, there was also the walker strand located at other three positions even though the distributions were all less than 15%. To initiate the walking, UV irradiation (2 h) was then introduced for the cleavage reaction of disulfide bond in stator strand. The sample was controlled at 4 °C during photoirradiation to decrease irradiation damage. The distribution ratios of pyrene-walker at four positions on the DNA tile indicating the movement of walker strand along stators were evaluated. AFM imaging was employed to confirm the irradiated samples and the results were all summarized in five histogram-graphs in Figure 2b (Table S2, Figure S2). After 2 h, the walker-S4 duplex was increased from 7% to ~ 34% while the walker-S1 duplex was decreased from initial ~ 65% to ~ 20%. In addition, the yield of the walker in position S2 and position S3 progressively changed in accordance with the walker's directional movement. And walker moving from S1 to S2 in our 2D walking system exhibited a relatively higher speed in a one-hour irradiation, when compared with previously reported photo-driven DNA motors.<sup>24</sup> This is probably because that the linear track on DNA tile might increase the probability of partially dissociated walking strand to associate with neighboring stators. The distribution ratios of the

walker changed over irradiation time, demonstrating that single-molecule movements on the DNA nanostructure were successfully driven by photoirradiation with directional control even though the movement of the walker strand cannot be controlled to stop at specified stator under the continuous irradiation of UV light.

The unidirectional movement of the walker transferring from S1 to S4 can be stimulated with three rate constants ( $k_1$ ,  $k_2$  and  $k_3$ ) in first-order, assuming that no hopping (more than one-sized step) occurs between neighboring sites and the backward movement is negligible (Figure 3a).<sup>29</sup> Meanwhile, it is also presumed that the reaction of photo-induced bond cleavage is much faster than the walking motions, which also can be negligible.<sup>26</sup> Therefore, four non-linear fitting equations were applied to analysis the dynamic movements of walking motor (see equations in Supporting Information), where the distribution ratio ( $y$ ) was corresponding to the walker occupied by each stator (the summary of the walker stepping from the former stator and the walker stepping forward to the next stator) under different irradiation time ( $t$ ). During UV irradiation over a period of two hours, the overall distribution ratios of walker occupying four stators are shown in Figure 3b. The data were fitted well into four nonlinear curves and the fitted value of walking rates were  $0.57 \text{ h}^{-1}$  ( $k_1$ ),  $0.80 \text{ h}^{-1}$  ( $k_2$ ) and  $0.79 \text{ h}^{-1}$  ( $k_3$ ), respectively. The value of  $k_1$  is smaller than  $k_2$  and  $k_3$ , most likely because S1, with two more bases, slowed down the walker's movement. The value of  $k_2$  and  $k_3$  were similar and also fitted well with the presumptive model. The slow fitted walking rates could probably be attributed to the low temperature ( $4 \text{ }^\circ\text{C}$ ) during the whole irradiation and walking process.

We next tried to directly observe the light-driven walker moving on the DNA origami under the scanning by high-speed AFM. After preparing the DNA tile containing walking strand and four stators, the sample was loaded onto a piece of freshly cleaved mica. High-speed AFM

imaging was carried out with photoirradiation in the UV range of  $\lambda = 330\text{--}380$  nm. A clear one-step movement of the pyrene-modified walker from one stator to the next was observed (Figure 4). The corresponding continuous kymograph is also shown in Figure 4b, showing the walker's changing position (Figure S3, Movie S1). Comparing position of walker at 40 s and 160 s, one-step distance was measured as  $\sim 7.5$  nm, which was close to the designed distance between two adjacent stators. In the consecutive walking track in the kymograph, the short walker-stator duplex on the DNA tile moved back and forth as Brownian motion in the beginning. Then, under UV irradiation, electron transfer-induced disulfide cleavage initiated a strand exchange reaction. In 90 s to 130 s, the motions of the walker were temporally stalled. An obvious position change of the walker occurred from 140 s  $\sim$  160 s. The walker formed the duplex with new stator again and maintained Brownian motion (170 s to 220 s). The direct visualization of walking movements driven by photoirradiation was successfully observed in our system even though the real-time statistics and kinetics analysis was still difficult to carry out under fast-scanning because of the fragility of the DNA tiles.

In summary, we have demonstrated a photocontrolled DNA walker moving on the designed DNA track constructed on the DNA origami surface. The stepwise movements of the walker on the DNA tile were fuelled by an optical source, and the autonomous unidirectional motions were regulated remotely. Furthermore, the real-time direct observation of the one-step forward motion of walker driven by photoirradiation was firstly visualized using high-speed AFM. The dynamically mechanical behaviors of single-stranded DNA in limited nanospace were successfully characterized in single molecule level. The photochemical reaction was successfully incorporated into the DNA origami-based molecular walkers. The photonic modification of DNA



based nanomaterials shows promise for biological applications such as cargo transport and manual configuration change of biomolecules in mesoscopic systems.

#### ASSOCIATED CONTENT

**Supporting Information.** Experimental procedures, DNA sequences, and additional AFM images. This material is available free of charge via the Internet at <http://pubs.acs.org>.

#### AUTHOR INFORMATION

##### Corresponding Author

endo@kuchem.kyoto-u.ac.jp (ME); hs@kuchem.kyoto-u.ac.jp (HS); tan@chem.ufl.edu (WT).

##### Present Addresses

l Department of Physics, Technische Universität München, München, Germany.

#### ACKNOWLEDGMENT

This work was supported by a Grant-in-Aid for Scientific Research on Innovative Areas "Molecular Robotics" (Grant Number 24104002) of MEXT, JSPS KAKENHI (Grant Numbers 15H03837, 24225005, 26620133), the Sekisui Chemical Research Grant, and the Kurata Memorial Hitachi Science and Technology Foundation. This work is also supported by grants awarded by the National Key Scientific Program of China (2011CB911000), NSFC grants (NSFC 21221003 and NSFC 21327009) and China National Instrumentation Program 2011YQ03012412 and by the National Institutes of Health (GM079359 and CA133086).

## REFERENCES

- (1) Greulich, K. O. *Chemphyschem* **2005**, *6*, 2458-2471.
- (2) Neuman, K. C.; Nagy, A. *Nat. Meth.* **2008**, *5*, 491-505.
- (3) Ishii, Y.; Yanagida, T. *Single Mol.* **2000**, *1*, 5-14.
- (4) Endo, M.; Sugiyama, H. *Acc. Chem. Res.* **2014**, *47*, 1645-1653.
- (5) Ando, T.; Kodera, N.; Takai, E.; Maruyama, D.; Saito, K.; Toda, A. *Proc. Nat. Acad. Sci.* **2001**, *98*, 12468-12472.
- (6) Ando, T.; Uchihashi, T.; Kodera, N. *Ann. Rev. Biophys.* **2013**, *42*, 393-414.
- (7) Rajendran, A.; Endo, M.; Sugiyama, H. *Angew. Chem. Int. Ed.* **2012**, *51*, 874-890.
- (8) Rothmund, P. W. K. *Nature* **2006**, *440*, 297-302.
- (9) Endo, M.; Yang, Y.; Sugiyama, H. *Biomat. Sci.* **2013**, *1*, 347-360.
- (10) Voigt, N. V.; Tarring, T.; Rotaru, A.; Jacobsen, M. F.; Ravnsbaek, J. B.; Subramani, R.; Mamdouh, W.; Kjems, J.; Mokhir, A.; Besenbacher, F.; Gothelf, K. V. *Nat. Nanotechnol.* **2010**, *5*, 200-203.
- (11) Endo, M.; Yang, Y.; Suzuki, Y.; Hidaka, K.; Sugiyama, H. *Angew. Chem. Int. Ed.* **2012**, *51*, 10518-10522.
- (12) Rajendran, A.; Endo, M.; Hidaka, K.; Sugiyama, H. *J. Am. Chem. Soc.* **2012**, *135*, 1117-1123.
- (13) Sannohe, Y.; Endo, M.; Katsuda, Y.; Hidaka, K.; Sugiyama, H. *J. Am. Chem. Soc.* **2010**, *132*, 16311-16313.
- (14) Endo, M.; Hidaka, K.; Sugiyama, H. *Org. Biomol. Chem.* **2011**, *9*, 2075-2077.
- (15) Suzuki, Y.; Endo, M.; Katsuda, Y.; Ou, K.; Hidaka, K.; Sugiyama, H. *J. Am. Chem. Soc.* **2013**, *136*, 211-218.

- (16) Wickham, S. F. J.; Bath, J.; Katsuda, Y.; Endo, M.; Hidaka, K.; Sugiyama, H.; Turberfield, A. J. *Nat. Nanotechnol.* **2012**, *7*, 169-173.
- (17) Wickham, S. F. J.; Endo, M.; Katsuda, Y.; Hidaka, K.; Bath, J.; Sugiyama, H.; Turberfield, A. J. *Nat. Nanotechnol.* **2011**, *6*, 166-169.
- (18) Yang, Y.; Endo, M.; Suzuki, Y.; Hidaka, K.; Sugiyama, H. *Chem. Comm.* **2014**, *50*, 4211-4213.
- (19) Suzuki, Y.; Endo, M.; Yang, Y.; Sugiyama, H. *J. Am. Chem. Soc.* **2014**, *136*, 1714-1717.
- (20) Yang, Y.; Endo, M.; Hidaka, K.; Sugiyama, H. *J. Am. Chem. Soc.* **2012**, *134*, 20645-20653.
- (21) Lund, K.; Manzo, A. J.; Dabby, N.; Michelotti, N.; Johnson-Buck, A.; Nangreave, J.; Taylor, S.; Pei, R.; Stojanovic, M. N.; Walter, N. G.; Winfree, E.; Yan, H. *Nature* **2010**, *465*, 206-210.
- (22) Liber, M.; Tomov, T. E.; Tsukanov, R.; Berger, Y.; Nir, E. *Small* **2015**, *11*, 568-575.
- (23) Gu, H.; Chao, J.; Xiao, S.-J.; Seeman, N.C. *Nature* **2010**, *465*, 202-205.
- (24) You, M.; Chen, Y.; Zhang, X.; Liu, H.; Wang, R.; Wang, K.; Williams, K. R.; Tan, W. *Angew. Chem. Int. Ed.* **2012**, *51*, 2457-2460.
- (25) You, M.; Huang, F.; Chen, Z.; Wang, R.-W.; Tan, W. *ACS nano* **2012**, *6*, 7935-7941.
- (26) You, M.; Zhu, Z.; Liu, H.; Gulbakan, B.; Han, D.; Wang, R.; Williams, K. R.; Tan, W. *ACS Appl. Mater. Interfaces* **2010**, *2*, 3601-3605.
- (27) Saffarian, S.; Collier, I. E.; Marder, B. L.; Elson, E. L.; Goldberg, G. *Science* **2004**, *306*, 108-111.
- (28) Mai, J.; Sokolov, I. M.; Blumen, A. *Phys. Rev. E* **2001**, *64*, 011102.
- (29) Bath, J.; Green, S. J.; Turberfield, A. J. *Angew. Chem. Int. Ed.* **2005**, *44*, 4358-4361.



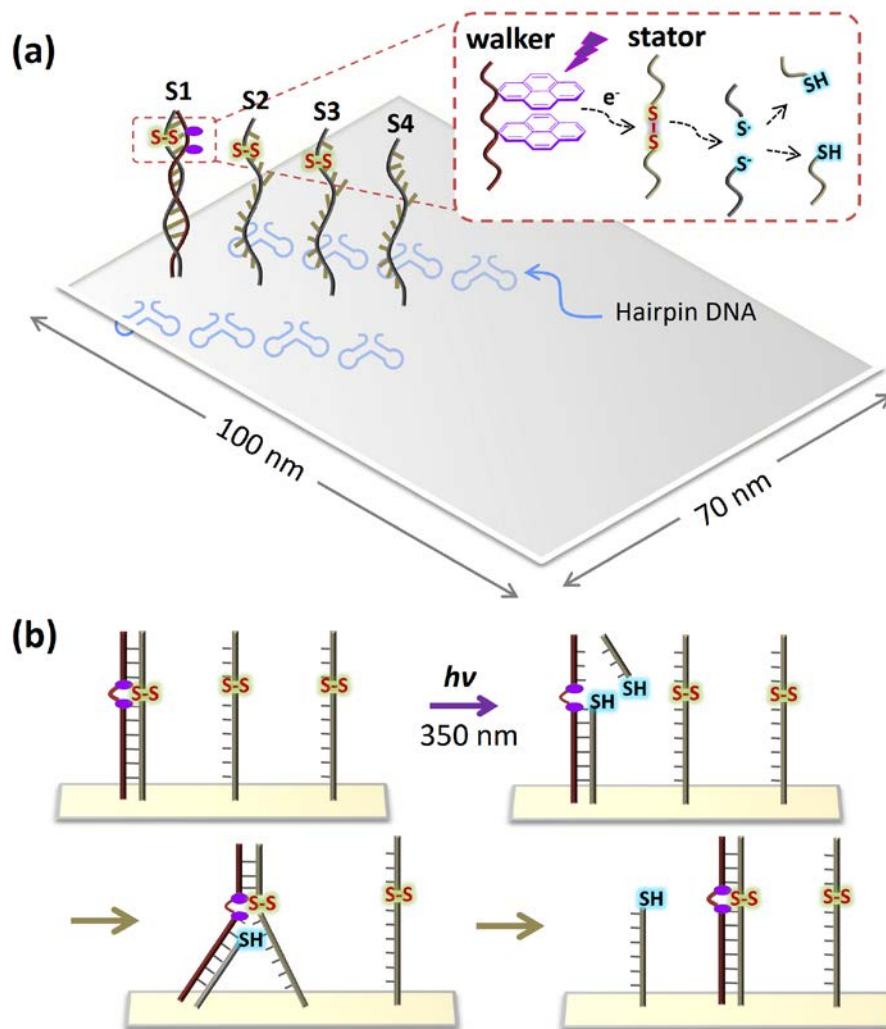


**Figure 1.** Schematic illustration of the light-driven walking system. (a) A rectangular DNA tile (70 nm  $\times$  100 nm) bearing four single-stranded stator strands (S1 to S4) assembled with a pyrene-modified walking strand; two rows of parallel hairpin loops (orange) along the walking track were on the opposite side of the DNA tile; dashed area: the cleavage of disulfide bond in the first walker-stator duplex by photoirradiation. (b) Illustration of the working mechanism of one-step motion of the walker; photolysis by irradiation at 350 nm initiates the strand-exchange reaction, resulting in migration of the walker from the cleaved stator strand to the next intact neighboring stator strand with directional control.

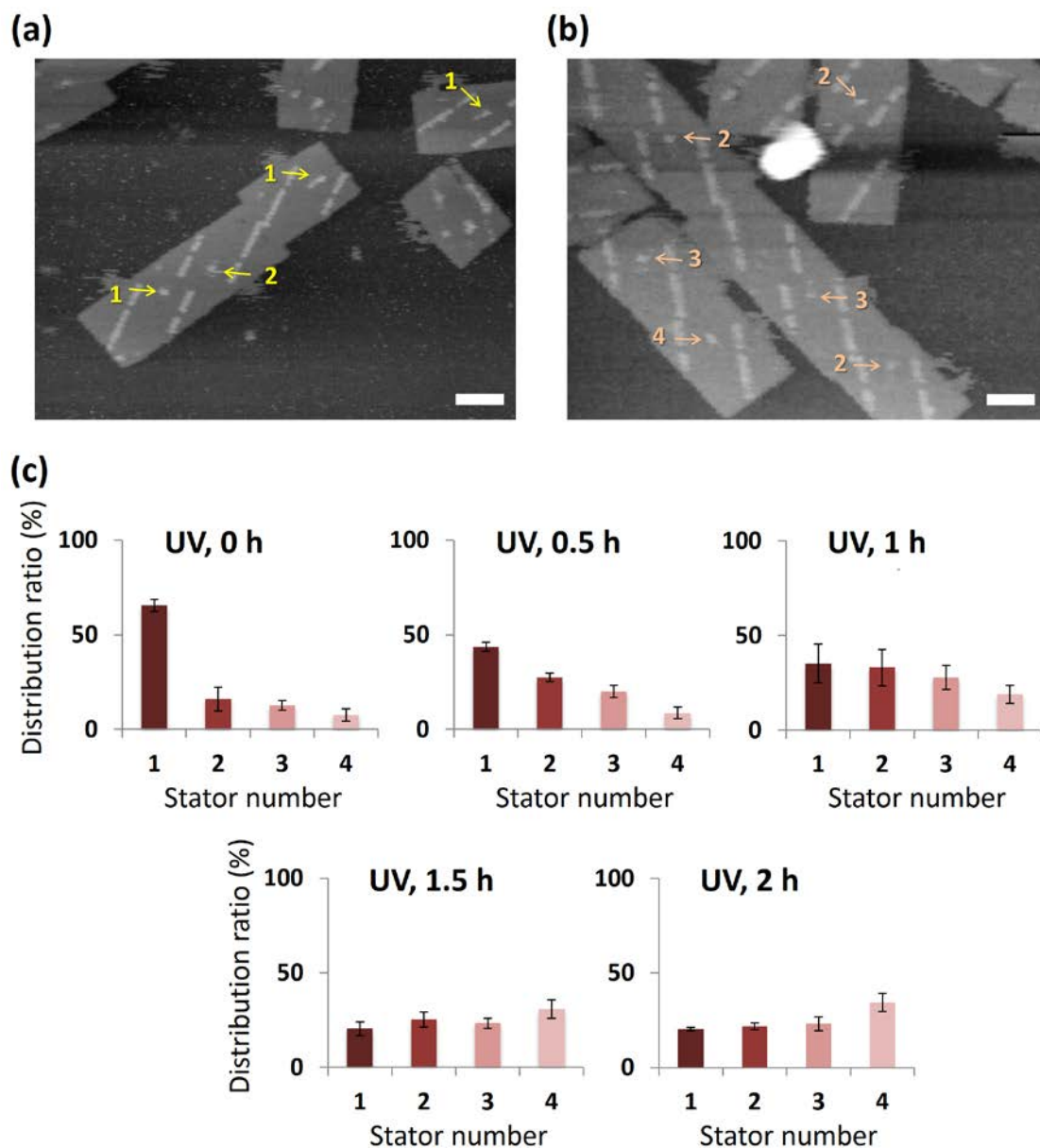


**Figure 2.** Light-powered movement of pyrene-modified walkers on DNA tile. AFM images of the DNA walking system showing the walker at the initial state (a) and after photoirradiation for 1.5 h at 4 °C (b). The positions are indicated by arrows and determined by using DNA hairpins as reference position markers; scale bars: 50 nm. (c) The distribution of the walker on four positions of the DNA tile was determined by AFM under different UV irradiation times; irradiation condition: 350 nm, 4 °C. Error bars (S.D.) were obtained from experiments repeated three times.

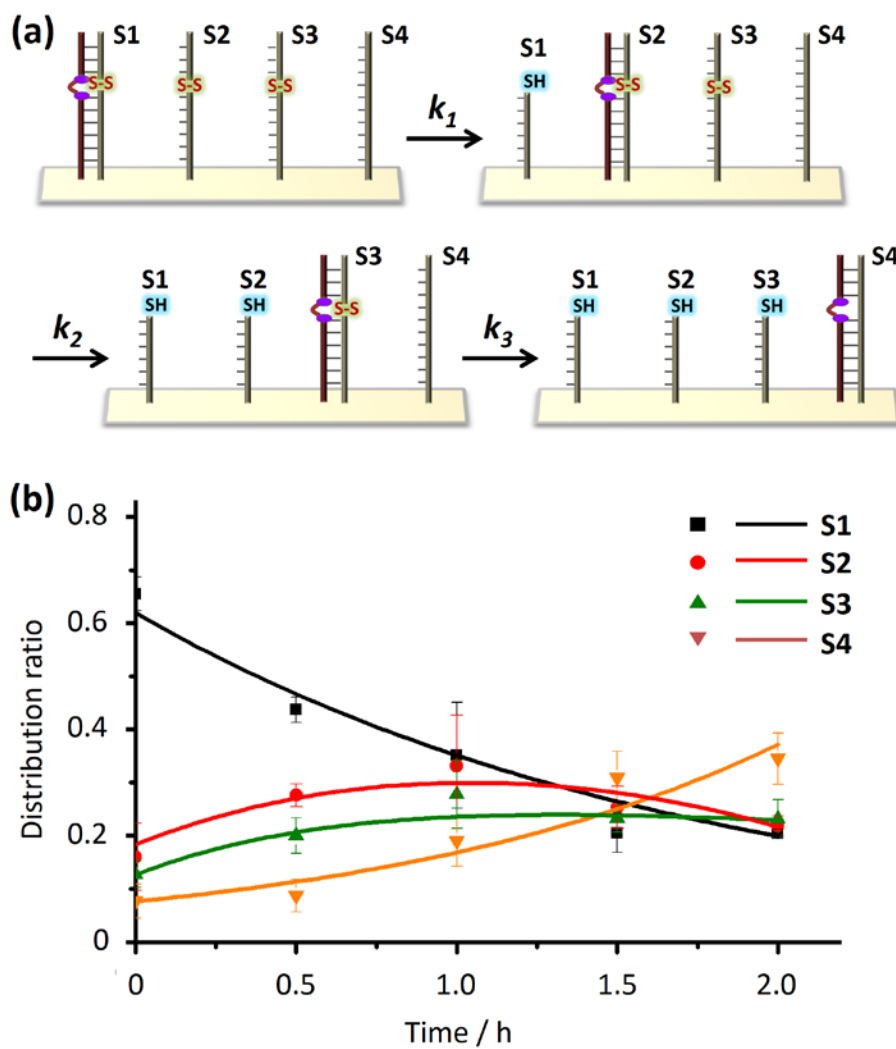


**Figure 3.** Kinetics analysis of walker movement on DNA tile. (a) Three-step movement of the walker from S1 to S4 along a linear track. (b) The data fitting for estimating the walking rates. For the fitting, distribution ratios of the walker at four respective stators in UV irradiation time were used. Irradiation condition: 350 nm, 4 °C. The error bars (S.D.) were obtained from experiments repeated three times.

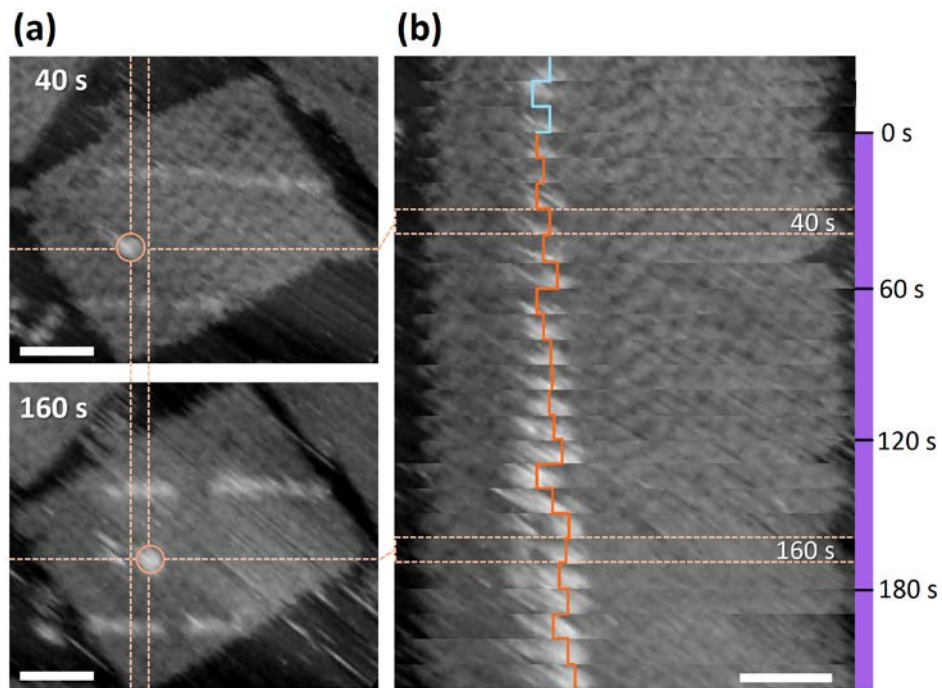


**Figure 4.** Direct visualization by HS-AFM of light-driven DNA walker's one-step motion. (a) Two representative AFM images of one-step forward motion of the DNA walking system at two time points. (b) Kymograph is the stack of frames from AFM images after introducing UV irradiation (time scale specific for irradiation is marked on the right side in seconds). The positions of the walker-stator duplex were imaged as the highest spot on the DNA tile, which were joined together by blue (before UV irradiation) and orange lines (during UV irradiation). Scanning speed: 0.1 frames/sec. UV irradiation: 350 nm, room temperature. Scale bars: 30 nm.



TOC Figure

